NJC

ROYAL SOCIETY OF CHEMISTRY

PAPER

View Article Online
View Journal | View Issue

Cite this: *New J. Chem.*, 2023, **47**, 12718

Copper diaryl-dithiocarbamate complexes and their application as single source precursors (SSPs) for copper sulfide nanomaterials†

Jagodish C. Sarker, [ab] Xiang Xu,[a] Firoz Alam, [c] Rosie Nash, [a] Suwimon Boonrungsiman,[d] David Pugh, [a] Jeremy K. Cockcroft, [e] David J. Lewis [c] and Graeme Hogarth *[a]

Received 26th April 2023,
Accepted 11th June 2023

DOI: 10.1039/d3nj01918g

rsc.li/njc

Copper diaryl-dithiocarbamate (DTC) complexes have been prepared including Cu(II) species, $[Cu(S_2CNAr_2)_2]$, and Cu(I) species $[Cu\{S_2CN(p\text{-tolyl})_2\}]_n$ and $[Cu\{S_2CN(p\text{-tolyl})_2\}(PPh_3)_2]$ with some examples being characterised by single crystal diffraction. CV measurements show that, like the dialkyl-analogues, $[Cu(S_2CNAr_2)_2]$ can be both oxidised and reduced, but while oxidation is reversible, reduction is irreversible and results from loss of a DTC ligand. Both Cu(II) and Cu(I) complexes $[Cu\{S_2CN(p\text{-}MeC_6H_4)_2\}_2]$ and $[Cu\{S_2CN(p\text{-}MeC_6H_4)_2\}]_n$ have been used as single source precursors to prepare covellite (CuS) or digenite ($Cu_{1.8}S$) nanoparticles in oleylamine.

1 Introduction

Copper sulfides ($Cu_{2-x}S$) are an important class of materials[1–6] especially for biological applications as both elements are biocompatible. A wide range of crystalline phases are known including Cu_2S (chalcocite), $Cu_{1.8}S$ (digenite), $Cu_{1.94}S$ (djurleite) and CuS (covellite), all of which are p-type semiconductors with band gaps of *ca.* 1.2 eV and can exhibit quantum confinement. Further, CuS, with its anisotropic p-type conductivity and carrier concentration of *ca.* 3×10^{27} m^{-3} is an excellent candidate for plasmonic applications in the near-infrared.[7–9]

Due to their ease of formation from cheap and readily available starting materials, and the ability of dithiocarbamate (DTC) ligands to form stable complexes with all of the d-block elements,[10] DTC complexes have been extensively utilised as single source precursors (SSPs) towards transition metal sulfides.[11] Cu(II) bis(dialkylDTC) complexes, $[Cu(S_2CNR_2)_2]$, have been previously employed to prepare binary, tertiary and quaternary copper-containing sulfides,[11,12] and they are especially applicable to the preparation of quantum dots (QDs). In 2003, Burda and co-workers reported that decomposition of $[Cu(S_2CNEt_2)_2]$ in a TOP/TOPO mixture at 250 °C *via* the heat-up (HU) method in the presence of added sulfur afforded $Cu_{1.8}S$ QDs[13] and soon after this Alivisatos decomposed the same SSP in mixture of dodecanethiol and oleic acid to produce Cu_2S QDs with an average size of 5.4 nm.[14,15] Decomposition of $[Cu(S_2CNEt_2)_2]$ in oleylamine (OLA) was first reported by Hu and co-workers who used a hot-injection (HI) method (300 °C) to generate relatively large $Cu_{1.8}S$ nanomaterials with an average diameter of *ca.* 70 nm and thickness of *ca.* 13 nm.[16] Lowering the decomposition temperature to 280 °C and adding oleic acid to the mixture allowed access to smaller $Cu_{1.8}S$ with a mean diameter of *ca.* 20 nm.[17] Other dialkyl SSPs have also been used, for example Wang and co-workers decomposed $[Cu(S_2CNBu_2)_2]$ by HI into a mixture of OLA, octadecane and dodecanethiol at 190 °C to give $Cu_{1.75}S$ nanocrystals with an average diameter of 9 nm.[18]

However, since in all these cases, the decomposition of $[Cu(S_2CNR_2)_2]$ occurs above 180 °C,[13–19] a temperature above which CuS (covellite) undergoes sulfur loss, this approach is not generally suitable for covellite formation. A current theme of our research is the identification of copper and sulfur containing SSPs that decompose at relatively low temperatures, allowing access to covellite QDs. In this regard we recently reported that $[Cu\{S_2CN(CH_2CO_2H)_2\}_2]$ decomposes in water at temperatures as low as 90 °C to give covellite nanospheres of diameter of 8 ± 1 nm, which further aggregate into larger hollow spheres with diameters of *ca.* 100 ± 40 nm.[20]

[a] *Department of Chemistry, King's College London, Britannia House, 7 Trinity Street, London SE1 IDB, UK. E-mail: graeme.hogarth@kcl.ac.uk*
[b] *Department of Chemistry, Jagannath University, Dhaka 1100, Bangladesh*
[c] *Department of Materials, University of Manchester, Oxford Road, Manchester M13 9PL, UK*
[d] *Centre for Ultrastructural Imaging, King's College London, New Hunt's House, London SE1 1UL, UK*
[e] *Department of Chemistry, University College London, 20 Gordon Street, London WC1H 0AJ, UK*

† Electronic supplementary information (ESI) available. CCDC 2258923–2258925. For ESI and crystallographic data in CIF or other electronic format see DOI: https://doi.org/10.1039/d3nj01918g

In developing the general use of DTC complexes as SSPs, we noted that diaryl-derivatives of the form $[M(S_2CNAr_2)_n]$ have received relatively little attention[10] despite the expectation that the N–C(sp^2) bond might be weaker than an analogous N–C(sp^3) bond, and thus they may serve as useful low temperature SSPs. The simplest copper example, namely $[Cu(S_2CNPh_2)_2]$, has been briefly reported[21,22] but synthetic details, characterisation data and thermal stability studies were lacking. We recently reported a development of the method of Snaith and co-workers[23] for the preparation of a range of salts, LiS_2CNAr_2, which are air and moisture stable and allow ready access to diaryl-DTC complexes.[24] Herein we report the preparation of a small series of copper diaryl-DTC complexes, accessing both the Cu(II) and Cu(I) state, and investigate the use of selected examples as SSPs for the synthesis of copper sulfides under a range of decomposition conditions. While this work was in progress, Freitag and co-workers reported the synthesis of $[Cu(S_2CNPh_2)_2]$ (**2a**) *via* a similar method.[25]

2 Results and discussion

2.1 Synthesis of $[Cu(S_2CNAr_2)_2]$ (2a–g)

Addition of $CuCl_2$ to two equivalents of diaryl-DTC salts **1a–g**[24] in water resulted in the immediate formation of a brown precipitate which, following simple work up (see Experimental section), afforded dark brown $[Cu(S_2CNAr_2)_2]$ (**2a–g**) in good yields (Scheme 1). Most of these complexes are soluble in polar organic solvents, their solubility increasing with increased functionalization of the aryl groups. Slow mixing of saturated CH_2Cl_2 or $CHCl_3$ solutions with hexanes, followed in some cases by slow solvent evaporation after mixing, gave **2a–g** as black crystals. Elemental analysis, IR and mass spectra are commensurate with the proposed structures, albeit they often crystallize with chlorinated solvent in the lattice. To confirm the Cu(II) oxidation state we performed magnetic susceptibility measurements on **2a–c**, magnetic moments (μ_{eff}) ranging from 2.08–2.92 BM, being slightly higher than for related dialkyl-DTC complexes ($\mu_{eff} \sim 1.9$).

2.2 Molecular structures of $[Cu\{S_2CN(p\text{-}MeC_6H_4)_2\}_2]$ (2b) and $[Cu\{S_2CN(p\text{-}MeOC_6H_4)_2\}_2]$ (2c)

$[Cu(S_2CNR_2)_2]$ adopt three structural types in the solid state.[10,12] Two are common, namely a dimeric structure in which Cu(II) centres are held together by intermolecular Cu–S interactions, or discrete square-planar $[Cu(S_2CNR_2)_2]$ centres. The third is unique to $[Cu(S_2CNMe_2)_2]$ which forms a coordination polymer with approximately octahedral Cu(II) centres.[26] Generally, bulky substituents push the system towards a discrete square-planar structure, and this (to some extent) allows a comparison of the steric effects of alkyl *vs.* aryl substituents.

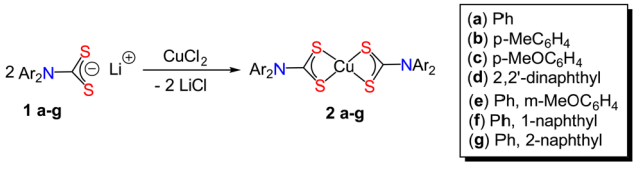

Scheme 1 Synthesis of $[Cu(S_2CNAr_2)_2]$ (**2a–g**)

Molecular structures of **2b-c** were elucidated by X-ray crystallography (Fig. 1 and 2). Both complexes adopt a centrosymmetric dimeric structure and all Cu–S bond lengths and intermolecular Cu–Cu and Cu–S bond distances and S–Cu–S angles are in agreement with those in dimeric dialkyl-DTC complexes.[10,12] The aryl rings lie approximately perpendicular to the CuS_4 plane showing that they are not conjugated with the electronically delocalised $CuNCS_2$ moiety, something we have seen in other complexes of these ligands.[24]

2.3 Electrochemical studies of $[Cu\{S_2CN(p\text{-}MeC_6H_4)_2\}_2]$ (2b)

A key feature of dialkyl-DTC complexes $[Cu(S_2CNR_2)_2]$ is their electrochemical conversion to the Cu(III) and Cu(I) complexes, $[Cu(S_2CNR_2)_2]^+$ and $[Cu(S_2CNR_2)_2]^-$ respectively.[21] Oxidation is both chemically and electrochemically reversible and Cu(III) cations have been isolated and crystallographically characterised,[27–29] but Cu(I) complexes $[Cu(S_2CNR_2)_2]^-$ rapidly lose a DTC anion to give tetrahedral Cu(I) clusters $[Cu(\mu^3\text{-}S_2CNR_2)]_4$.[30–32] To compare with the dialkyl-DTC derivatives, the electrochemical behavior of **2b** was investigated by cyclic voltammetry (CV) in at room temperature in MeCN (Fig. 3).

A reversible oxidation is seen at *ca.* 0.1 V *vs.* $Fc^{+/0}$ consistent with the reversible formation of $[Cu\{S_2CN(p\text{-}MeC_6H_4)_2\}_2]^+$. This behaviour is very similar to that observed for related dialkyl-DTC analogues[21] and the square-planar Cu(III) complexes $[Cu(S_2CNR_2)_2]^+$ can be synthetically accessed and analyzed in the solid-state.[27–29] We made no attempt to isolate $[Cu\{S_2CN(p\text{-}MeC_6H_4)_2\}_2]^+$, but while this work was in progress a small number of single crystals of $[Cu(S_2CNPh_2)_2][I_3]$ were isolated from the reaction of **2a** and CuI.[25] The reduction of **2b** in MeCN shows only slight reversibility across a range of scan rates. To try and stabilise the Cu(I) anion generated, we also carried out CVs of **2b** in CH_2Cl_2 at −78 °C (Fig. S1, ESI†) but even under these conditions, reduction was effectively irreversible. This differs from the analogous dialkyl-DTC derivatives and shows that dithiocarbamate loss from $[Cu(S_2CNAr_2)_2]^-$ is facile. This likely results from the relatively poor donor ability of diaryl *vs.* dialkyl-DTCs. We do not see any back-oxidation of the generated neutral Cu(I) complex, likely due to its insolubility in both MeCN and CH_2Cl_2 (see next section) (Scheme 2).

2.4 Synthesis of copper(I) diarylDTC complexes and molecular structure of $[Cu\{S_2CN(p\text{-}MeC_6H_4)_2\}(PPh_3)_2]$ (4)

In copper sulfides, copper is predominantly in the +1 oxidation state.[2] Consequently, reduction of Cu(II) to Cu(I) is a key step in the decomposition of Cu(II) DTC SSPs to nanoscale copper sulfides. We have seen electrochemically that the Cu(I) state is accessible for diaryl-DTCs and thus we attempted the preparation of selective examples in order to compare with their Cu(II) analogues. We targeted $[Cu\{S_2CN(p\text{-}MeC_6H_4)_2\}]_n$ (**3**) as **2b** has better solubility than **2a** in a range of common solvents and the methyl group is an effective NMR handle. We initially followed a procedure for the synthesis of $[Cu(\mu_3\text{-}S_2CNBu_2)]_4$

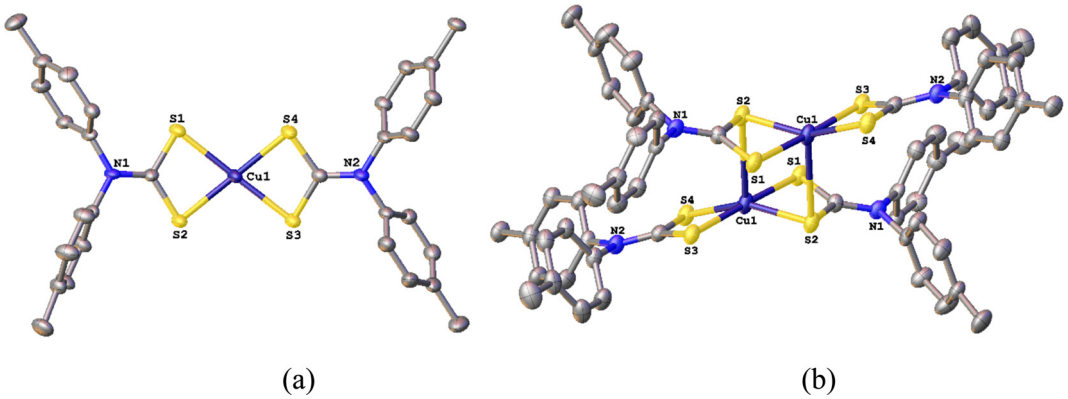

Fig. 1 Representations of the molecular structure of $[Cu\{S_2CN(p\text{-}MeC_6H_4)_2\}_2]$ (**2b**) showing (a) a single square-planar molecule, (b) linking to give dimeric units (H atoms omitted for simplification).

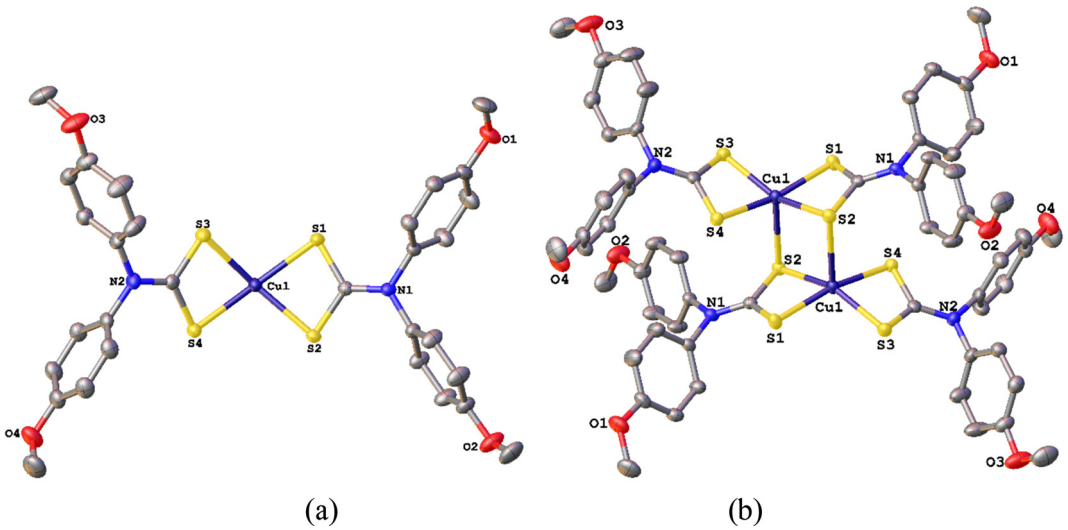

Fig. 2 Representations of the molecular structure of $[Cu\{S_2CN(p\text{-}MeOC_6H_4)_2\}_2]$ (**2c**) showing (a) a single square-planar molecule, (b) linking to give dimeric units.

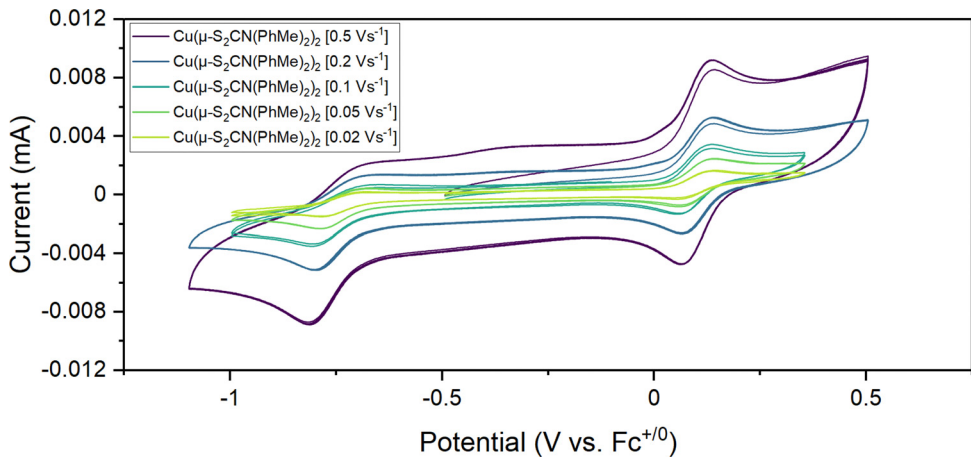

Fig. 3 CVs of **2b** (1 mM) in 0.1 M $[Bu_4N][PF_6]$ in MeCN at a scan rates of 0.02–0.5 V s^{-1}.

previously used in our group,[31] namely the addition of activated Cu powder to **2b**, but this was unsuccessful. However, the slow (*ca.* 24 h) reaction of **1b** and CuCl in a MeOH–CH_2Cl_2 mixture under an inert atmosphere, led to a gradual darkening of the

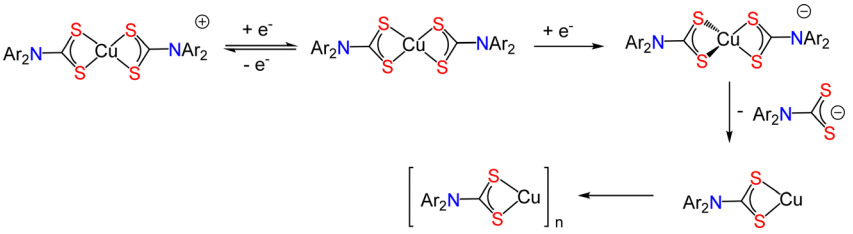

Scheme 2 Redox chemistry of $[Cu(S_2CNAr_2)_2]$ (**2b**) as interpreted from CVs.

pale yellow solution and deposition of a dark yellow precipitate which after work-up afforded a yellow powder that we (tentatively) assign as $[Cu\{S_2CN(p\text{-}MeC_6H_4)_2\}]_\infty$ (**3**) (*ca.* 96% yield). To expedite the process, we attempted the same reaction in water (in air) but this led only to formation of **2b**. Complex **3** has poor solubility in a range of common organic solvents, which is surprising given the high solubility of $[Cu(\mu_3\text{-}S_2CNBu_2)]_4$,[31] and this has precluded full purification and characterization. It is sparingly soluble in $CDCl_3$ and the $^{13}C\{^1H\}$ NMR spectrum shows a thioureide signal at δ 204.5 ppm, but there are three methyl resonances (21.1, 21.0 and 20.9 ppm), while the ^1H NMR spectrum shows a multiplet at δ 2.32 suggesting a range of methyl environments (Fig. S2 and S3, ESI†). Thus, considering the spectroscopic data and poor solubility, we suggest that **3** has a more complex structure than the tetrahedral seen for dialkyl-derivatives, likely being a coordination polymer as has been found for related xanthate complexes, $[Cu(S_2COR)]_\infty$ (R = Me, ^{i}Pr)[33,34] or even a mixture of oligomers. It does (slowly) dissolve in d^6-dmso to give a dark yellow solution, but the $^{13}C\{^1H\}$ NMR spectrum does not show a low-field thioureide signal (Fig. S4 and S5, ESI†). We believe that dissolution likely leads to formation of mononuclear species $[Cu\{S_2CN(p\text{-tolyl})_2\}(dmso)_n]$, as we have recently noted similar behaviour for Cu(I) complexes of primary amine-derived DTCs.[35]

It has been reported that addition of PPh_3 to $[Cu(S_2CNR_2)]_4$ in MeCN affords bis(phosphine) adducts $[Cu(S_2CNR_2)(PPh_3)_2]$.[36] Addition of two equivalents of PPh_3 to a CH_2Cl_2 suspension of **3** afforded $[Cu\{S_2CN(p\text{-}MeC_6H_4)_2\}(PPh_3)_2]$ (**4**) in *ca.* 39% yield. Cu(I) bis(phosphine) complexes can also be prepared upon addition of DTC salts to $[(Ph_3P)_2Cu(NO_3)]$[37,38] and we found this to be the simplest and highest yielding route to **4**. Addition of a CH_2Cl_2 solution of $[(Ph_3P)_2Cu(NO_3)]$ to **1b** in MeOH afforded yellow crystals of **4** in *ca.* 90% yield. Somewhat surprisingly, **4** was also formed upon addition of a slight excess of PPh_3 to CH_2Cl_2 solutions of **2b**, the PPh_3 acting as both a reducing agent and coordinating ligand to the Cu(I) centre. Attempts to carry out the same reduction with $[Cu(S_2CNBu^i_2)_2]$ failed, with no discernable change being seen to the dark brown solution even after prolonged timeframe (weeks). This difference in reactivity may result from the slightly lower reduction potential of **2b** *vs.* $[Cu(S_2CNBu^i_2)_2]$, and also the rapid loss of DTC from $[Cu(S_2CNAr_2)_2]^-$. This chemistry is summarized in Scheme 3.

Spectroscopic data for **4** are consistent with its formulation and we have characterized it by X-ray crystallography (Fig. 4). The Cu(I) center has a distorted tetrahedral geometry [τ'_4parameter = 0.81,[39] S1–Cu1–S2 75.90(4), P1–Cu1–P2 115.97(5)°] and Cu–S bond distances [2.3836(14) and 2.4087(14) Å] reflect a symmetric binding of the DTC ligand. In solution, like many Cu(I) d^{10} complexes, it is fluxional, and part dissociates. Thus, peaks in the NMR spectra are broad and appear alongside sharp minor peak(s) associated with ligand loss in solution. This is most clearly seen in the $^{31}P\{^1H\}$ NMR spectrum which primarily consists of a broad resonance at δ −0.8 ppm, but also contains a sharp singlet at 29.8 ppm (integrated ratio *ca.* 30 : 1) which we assign to $[Cu(PPh_3)_2]^+$. In the $^{13}C\{^1H\}$ NMR spectrum the characteristic thioureide carbon signal appears at δ 210.0 (Fig. S6–S8, ESI†).

2.5 Decomposition studies

For the decomposition studies we primarily focused on $[Cu\{S_2CN(p\text{-}MeC_6H_4)_2\}_2]$ (**2b**). We first investigated its decomposition by TGA (Fig. 5). It is stable up to *ca.* 250 °C and then undergoes rapid decomposition. This can be compared to $[Cu(S_2CNEt_2)_2]$ which only begins to decompose at *ca.* 290 °C,[40] confirming that Ar–N bond scission is more favourable than R–N cleavage. Further, solid-state decomposition of **2b** occurs

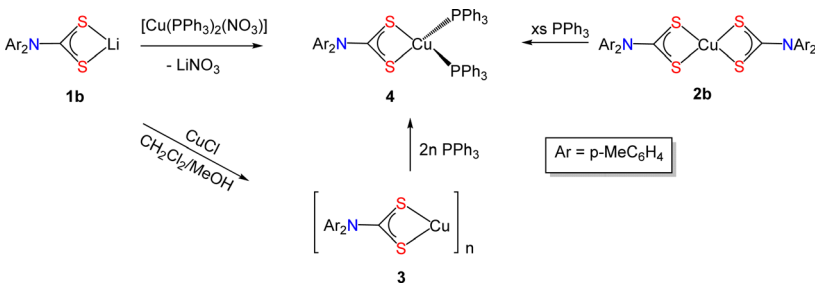

Scheme 3 Synthetic routes to $[Cu\{S_2CN(p\text{-}MeC_6H_4)_2\}(PPh_3)_2]$ (**4**).

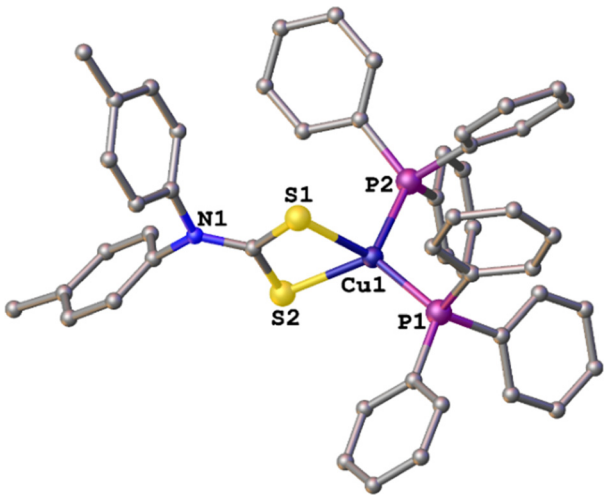

Fig. 4 The molecular structure of $[Cu\{S_2CN(p\text{-}MeC_6H_4)_2\}(PPh_3)_2]$ (**4**) (H atoms omitted for clarity).

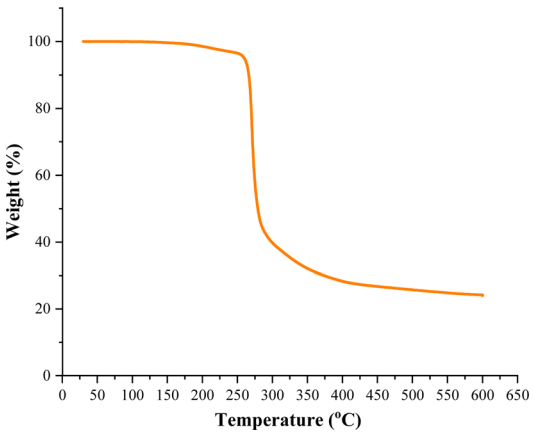

Fig. 5 TGA of $[Cu\{S_2CN(p\text{-}MeC_6H_4)_2\}_2]$ (**2b**).

in a single step, while for $[Cu(S_2CNEt_2)_2]$ a two-step decomposition profile is seen. The residual mass from **2b** (*ca.* 22%) is consistent with formation of a copper-rich phases such as Cu_2S or $Cu_{1.8}S$ but we have not confirmed this. The TGA suggests that **2b** would be unsuitable as a low temperature SSP, however, we have previously shown that in primary amines such as oleylamine (OLA), amine-exchange can occur to afford the primary amine complexes *in situ* and these decompose (*via* backbone deprotonation) at low temperatures.[11,41–43] Indeed, one of our justifications for studying diaryl-DTC complexes as SSPs was that this would be more facile than for dialkyl-DTC derivatives and as such provides a low temperature SSP route,[24] which is indeed the case as detailed later.

We studied the decomposition of **2b** under three different conditions namely, solvothermal heat-up (HU) and hot-injection (HI) in OLA and dry decomposition. For the HU process, **2b** was initially heated to 230 °C in OLA for 1 h. At room temperature, it was only partially soluble in OLA but at *ca.* 40–50 °C it fully dissolved. The dark brown solution generated

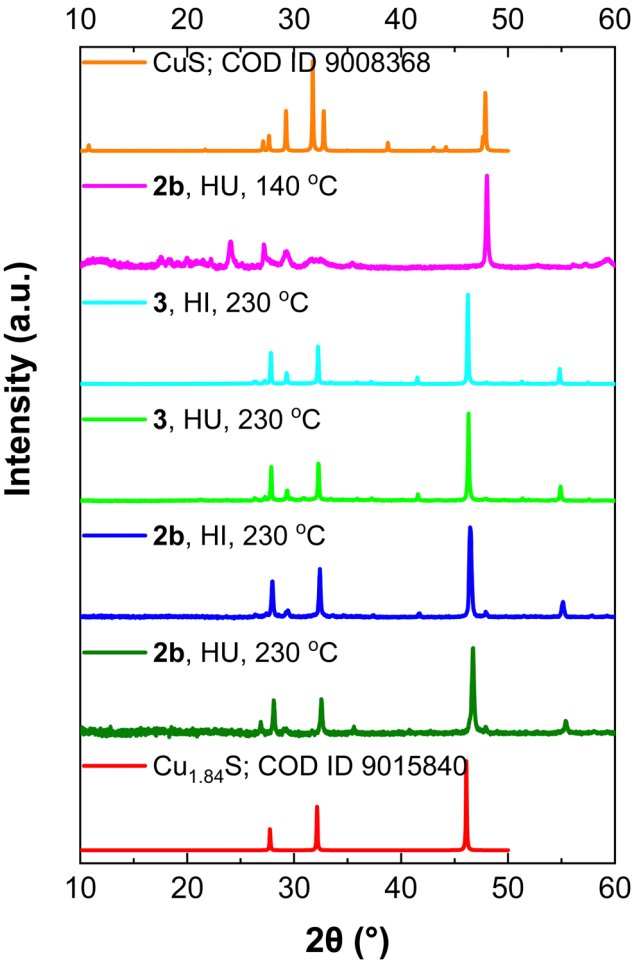

Fig. 6 Powder diffraction patterns of copper sulfides produced from SSPs **2b** and **3** by HU and HI decomposition methods.

upon dissolution remained unchanged until *ca.*180 °C, at which point the solution turned black. Heating was continued to 230 °C and held at this temperature for 1 h. After standard work up (see experimental section) a black solid was collected and dried in air. For HI, a warm (*ca.* 70 °C) OLA solution of **2b** was injected in OLA at 230 °C, the mixture turning black instantly. It was again held at this temperature for 1 h before cooling and work up. As shown by PXRD (Fig. 6) both HU and HI of **2b** in OLA produce $Cu_{1.8}S$ and the SAED pattern is consistent with this (Fig. S9, ESI†). As calculated by the Scherrer equation using full width half maxima (FWHM) (Table S2, ESI†), particles of *ca.* 35–36 nm are formed from HI and HU respectively. However, TEM images of the HU product (Fig. 7a and b) show rectangular particles with a significantly large average size of 88 ± 21 nm, highlighting the inaccuracy of the FWHM approach. We also studied the decomposition of **2b** at 140 °C *via* HU. The PXRD peaks associated with the formation of CuS (covellite) are observed although the spectrum is not very clean. Nevertheless, this observation, the decomposition of **2b** at well below its solid decomposition temperature provides further evidence of amine-exchange with likely intermediate generation of a primary amine complex that then decomposes rapidly.[10,41–43]

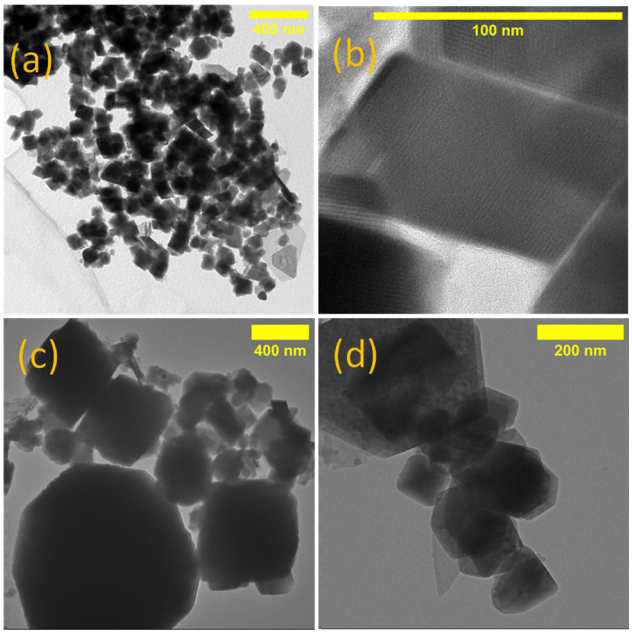

Fig. 7 TEM images of nanoparticles from (a) **2b** by HU, (b) the surface of a single rectangular particle, (c) **3** by HU and (d) **3** by HI.

The Cu(I) precursor, $[Cu\{S_2CN(p\text{-}MeC_6H_4)_2\}]_n$ (**3**) dissolves in OLA to afford a yellow-green solution, likely resulting from breakdown of the polymeric structure with coordination of one or more molecules of OLA to the Cu(I) centre. Upon heating to 100 °C the solution turned orange and at higher temperatures red (140 °C), brown (160 °C) and finally black at 200 °C. Heating was continued to 230 °C and maintained at this temperature for 1 h. After work up black nanocrystals of $Cu_{1.8}S$ were isolated. Formation of $Cu_{1.8}S$ from **3** was also seen using the HI method, the yellow-green OLA solution turning black immediately upon injection in OLA at 230 °C. TEM images reveal that particles produced from **3** by both HU and HI are comparatively larger than those from **2b** and further they are irregular in morphology/dimension with lengths of 90 nm–1 μm. From the colour changes it seems that, while Cu(II) and Cu(I) SSPs **2a** and **3** respectively give the same nanomaterials, their decomposition pathways and nucleation mechanism(s) may differ significantly, with the Cu(I) complex displaying enhanced stability.

We also carried out the dry thermolysis of **2b**, a powdered sample being heated to 450 °C for 1 h under argon. This afforded a black powder shown by SEM to consist of worm-like nanoparticles of average size 20 nm (Fig. S10, ESI†). The PXRD (Fig. S11, ESI†) proved hard to interpret, showing a complex mixture that we have found difficult to fully assign and possibly contains both copper sulfides and copper oxides. EDX spectroscopic mapping (Fig. S12) shows that the proportion of Cu and S are 77.0 and 23.0% (by weight).

3 Summary and conclusions

In this contribution we have shown that the synthesis of copper complexes of diaryl-dithiocarbamates is relatively straightforward, and their properties are broadly in line with those of the extensively studied dialkyl-derivatives.[12] Thus, both Cu(II) and Cu(I) derivatives have been fully characterised and combined with the recent publication on the molecular structure of the Cu(III) complex $[Cu(S_2CNPh_2)_2][I_3]$[25] suggests that these complexes are now ripe for applications in both the materials science and biological domains. To this end, we have shown in some preliminary studies that they can be useful precursors to nanoscale copper sulfides.[10] While both Cu(II) and Cu(I) SSPs gave similar final results, namely the formation of nanoparticles of digenite ($Cu_{1.8}S$), it is clear from observing the colour changes and clarity of the solutions occurring during the heating process that at a molecular level different processes are occurring. This is likely a result of the different electrophilicities of the backbone carbon of the DTC in Cu(I) *vs.* Cu(II) complexes, the latter being more electrophilic due to the greater degree of thioureide resonance form adopted at the more Lewis acidic Cu(II) site (Scheme 4).[11]

This then leads to fast amine exchange, and it is the primary amine DTC complex that decomposes rapidly in a basic solution *via* elimination of RNCS and $[Ar_2NCS_2]^-$ (Scheme 5). This initially leads to the formation of covellite (CuS) and this was seen to result at 140 °C, albeit not cleanly, while at higher temperatures sulfur loss occurs to afford copper-rich phases, at 230 °C digenite being favoured.

To further substantiate this hypothesis, we have recently isolated some copper complexes containing primary amine derived DTC ligands, and while they are stable at elevated temperatures at pH 7 and below, under basic conditions they rapidly decompose even at 40 °C to afford very small nanoparticles of covellite.[35]

4 Experimental section

All solvents and chemicals were purchased from Sigma-Aldrich or Alfa Aesar and used without any further purifications. ^1H NMR and $^{13}C\{^1H\}$ NMR spectra were recorded on a Bruker Avance III 400 MHz spectrometer using residual protons from either d^6-dmso or $CDCl_3$ as solvents for reference. IR analyses were conducted using PerkinElmer Spectrum 2 FTIR, or Shimadzu Affinity IR spectrophotometer. Mass spectra were

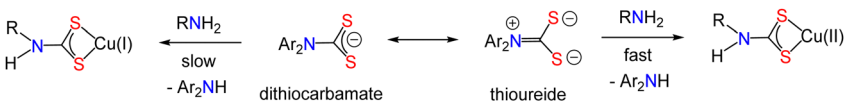

Scheme 4 DTC amine-exchange at Cu(I) and Cu(II) centres.

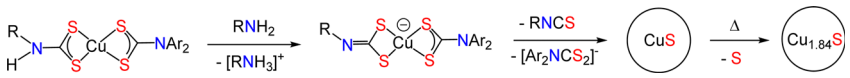

Scheme 5 Postulated decomposition pathways for copper diaryl-DTC complexes in OLA (RNH_2).

obtained by Micromass 70-SE spectrometer utilising Electrospray Ionisation (ESI†). Elemental analyses were performed by Flash 2000 Organic Elemental Analyzer of the Science Centre at London Metropolitan University. PXRD patterns were measured at University College London on a Bruker AXS D4 diffractometer using Cu Kα1 radiation. Diffraction patterns obtained were compared to database standards. TEM images were obtained using a JEOL-1010 microscope at 100 kV equipped with a Gatan digital camera. A 4 mL droplet of nanoparticle suspension ($CHCl_3$) was placed on a holey carbon-coated copper TEM grid and allowed to evaporate in air under ambient laboratory conditions for several minutes.

4.1 Synthesis and characterisation of $[Cu(S_2CNAr_2)_2]$ (2a–g)

$Li(S_2CNPh_2)$ (**1a**) (126 mg, 0.50 mmol) and $CuCl_2$ (33.61 mg, 0.25 mmol) were dissolved in water (10 mL) and stirred for 10 min at room temperature. A dark brown precipitate resulted which was collected by filtration, washed with water, and air dried to give **2a** (136 mg, 99% yield) as a dark brown solid. Similar scale and procedure were followed for **2b–g**.

2a (Ar = Ph): dark brown crystals, 136 mg, 99% yield. Elemental analysis: calcd for **2a**. $^1/_3CH_2Cl_2$: C, 54.50; H, 3.59; N, 4.83%. Found: C, 54.57; H, 3.38; N, 4.89%. IR (solid) (cm^{-1}): 614, 649, 693, 747, 1049, 1350, 1391, 1488. ESI-MS: *m*/*z* 550.98 (M^+, 100%). Magnetic susceptibility, μ_{eff}: 2.32 BM. **2b** (Ar = MeC_6H_4): dark brown crystals, 150 mg, 100% yield. Elemental analysis: calcd for $C_{30}H_{28}N_2S_4Cu$: C, 59.23; H, 4.64; N, 4.60%. Found: C, 59.11; H, 4.71; N, 4.72%. IR (solid) (cm^{-1}): 550, 762, 1034, 1046, 1351, 1506. ESI-MS: *m*/*z* 607 (^{63}Cu, M^+), 609 (^{65}Cu, M^+). Magnetic susceptibility, μ_{eff}: 2.08 BM. **2c** (Ar = *p*-$MeOC_6H_4$): dark brown, 100% yield. Elemental analysis: calcd for **2c**. $^1/_2CHCl_3$: C, 50.04; H, 3.92; N, 3.83%. Found: C, 50.74; H, 4.09; N, 3.82%. IR (solid) (cm^{-1}): 565, 598, 817, 1034, 1240, 1502. ESI-MS: *m*/*z* 671 (M^+, 100%). Magnetic susceptibility, μ_{eff}: 2.92 BM. **2d** (Ar = 2,2′-dinaphthyl): dark brown crystals, 110 mg, 59% yield. Elemental analysis: calcd for **2d**.$2CH_2Cl_2$: C, 57.30; H, 3.50; N, 3.04%. Found: C, 54.67; H, 3.39; N, 2.93%. IR (solid) (cm^{-1}): 474, 748, 770, 789, 1034, 1217, 1229, 1277, 1327, 1364, 1591. ESI-MS: *m*/*z* 751.04 (M^+). **2e** (Ar = Ph, *m*-$MeOC_6H_4$): dark brown crystals, 121 mg, 79% yield. Elemental analysis: calcd for **2e**. $^1/_3CH_2Cl_2$:C, 53.14; H, 3.88; N, 4.37%. Found: C, 53.13; H, 3.89; N, 4.32%. IR (solid) (cm^{-1}): 503, 621, 658, 735, 685, 696, 772, 835, 995, 1034, 1047, 1138, 1225, 1285, 1310, 1356, 1485, 1585, 1601. ESI-MS: *m*/*z* 611.00 (M^+). **2f** (Ar = Ph, 1-naphthyl): dark brown crystals, 131 mg, 80% yield. Elemental analysis: calcd for **2f**. $^1/_3CHCl_3$: C, 59.61; H, 3.55; N, 4.05%. Found: C, 59.66; H, 3.61; N, 3.99%. IR (solid) (cm^{-1}): 496, 527, 552, 609, 629, 664, 691, 727, 766, 777, 797, 1088, 1269, 1308, 1341, 1354, 1389, 1491, 1593. ESI-MS: *m*/*z* 651.20 (M^+). **2g** (Ar = Ph, 2-naphthyl): dark brown crystals,132 mg, 81% yield. Elemental analysis: calcd for **2g**. $^1/_3CHCl_3$: C, 59.61; H, 3.55; N, 4.05%. Found: C, 60.13; H, 3.68; N, 4.01%. IR (solid) (cm^{-1}): 476, 557, 664, 691, 731, 746, 789, 810, 1036, 1233, 1267, 1308, 1339, 1368, 1489, 1506, 1591. ESI-MS: *m*/*z* 651.11 (M^+).

4.2 Synthesis and characterisation of $[Cu\{S_2CN(p\text{-}MeC_6H_4)_2\}]_n$ (3)

1b (280 mg, 1 mmol) was dissolved in MeOH (5 mL) and mixed with a CH_2Cl_2 (5 mL) suspension of CuCl (100 mg, 1 mmol) under N_2 at room temperature. There was no immediate colour change, but the solution slowly turned from a pale to a darker yellow. The mixture was stirred overnight to afford a dark yellow suspension. The solvent was removed under reduced pressure and the residue was washed with MeOH (10 mL) and dried to give $[Cu\{S_2CN(p\text{-}MeC_6H_4)_2\}]_n$ (**3**) (321 mg, 96%). Yellow solid, 96% yield. Elemental analysis: calcd for **3**: C, 53.63; H, 4.20; N, 4.17%. Found: C, 53.27; H, 4.09; N, 4.39%.^{1}H NMR ($CDCl_3$, 400 MHz): δ 7.36–7.04 (br. m, 8 H), 2.32 (m, 6 H). $^{13}C\{^1H\}$ NMR ($CDCl_3$): δ 204.5, 144.8, 137.5, 130.2, 129.9, 129.8, 126.4, 125.7, 21.1, 21.0, 20.9.

4.3 Synthesis and characterisation of $[Cu\{S_2CN(p\text{-}MeC_6H_4)_2\}(PPh_3)_2]$ (4)

Three methods were used to prepare **4**. (i) A solution of $[(Ph_3P)_2Cu(NO_3)]$ (200 mg, 0.308 mmol) dissolved in CH_2Cl_2 (10 mL) was added to a solution of **1b** (86 mg, 0.308 mmol) in MeOH (10 mL). The mixture was stirred for 2 h at room temperature to give a pale-yellow solution. Volatiles were removed by rotary evaporator and the yellow residue was washed with water (2 × 10 mL) and dried over $MgSO_4$ to give **4** (240 mg, 90%). After recrystallization in CH_2Cl_2/MeOH, yellow crystals of **4** were obtained. (ii) **3** (178 mg, 0.5 mmol) was suspended in CH_2Cl_2 (10 mL) and PPh_3 (263 mg, 1.0 mmol) added. The solution stirred for 24 h at room temperature during which time a pale-yellow solution developed. The solvent was removed and the residue recrystallized in CH_2Cl_2/MeOH to give yellow crystals of **4** (172 mg, 39%). (iii) A slight excess of PPh_3 (330 mg, 1.25 mmol) was added to CH_2Cl_2 (20 mL) solution of **2b** (304 mg, 0.5 mmol). A slow discoloration of the brown solution occurred over *ca.* 20 h at room temperature and finally gave a pale-yellow solution. The solvent was removed by rotary evaporator and the residue recrystallized in CH_2Cl_2/MeOH gave yellow crystals of **4** (400 mg, 93%). Yellow crystals. Elemental analysis: calcd for **4**. CH_2Cl_2: C, 66.06; H, 4.90; N, 1.48%. Found: C, 66.23; H, 4.99; N, 1.47%.^{1}H NMR ($CDCl_3$, 400 MHz): δ 7.32 (m, 19H), 7.19 (t, J = 8 Hz, 15H), 7.10 (br. m, 4H), 2.28 (s, 6H). $^{13}C\{^1H\}$ NMR ($CDCl_3$,125 MHz): δ 210.0, 134.6, 134.3, 134.0, 133.9, 132.3, 1.32.2, 129.7, 129.3, 128.7, 128.6, 128.3, 127.7, 21.3. $^{31}P\{^1H\}$ NMR ($CDCl_3$, 161 MHz):

δ 29.8 (s, 0.03 P, $[Cu(PPh_3)_2]^+$), −0.8 (br, w 1 P). ESI-MS: 860.15 (M^+ + 1).

4.4 Single crystal X-ray diffraction

The EPSRC UK National Crystallography Service at the University of Southampton collected crystallographic data for **2b** and **4**.[44] Hardware used for **2b**: a Rigaku 007 HF diffractometer (Cu K_α radiation, 1.54178 Å); for **4**: a Rigaku FR-E+ diffractometer (Mo-K_α radiation, 0.71073 Å). Both were equipped with HF Varimax confocal mirrors, a UG2 universal goniometer, HyPix-6000HE detector, and an Oxford Cryosystems low-temperature device. Datasets were processed using CrysAlisPro[45] solutions were solved and refined using Olex-2.[46] Data for **2c** were collected at University College London using a SuperNova, Dual, Cu at zero, Atlas diffractometer. For all, Olex2[46] was used, structures being solved with the Olex2.solve[47] structure solution program using charge flipping and refined with the SHELXL[48] refinement package using least squares minimization. CCDC reference numbers 2258923 (**2b**), 2258924 (**2c**) and 2258925 (**4**) contain the crystallographic data in CIF format which is summarized in Table S1 (ESI†). Despite multiple recrystallisation attempts, all crystals of **4** were found to be twinned. The best-diffracting crystal was a split crystal and the high-angle diffraction was not very strong. This gave poor data metrics including low completeness, high R_{int} and low I/σ ratio.

4.5 Solvothermal heat-up (HU) process

2b (25 mM) was added to OLA (20 mL) in a three-neck round bottom flask attached to a condenser and evacuated and refilled with N_2 repeatedly for 15 min. The solution was heated to 230 °C and held there for 1 h. The mixture was slowly cooled to room temperature, whereupon MeOH (80 mL) was added with stirring. The mixture was centrifuged, and the solution decanted to give the resultant nanoparticles. This procedure was repeated four times (3 × 80 mL MeOH, 1 × 80 mL CH_2Cl_2) and following this the material was air-dried.

4.6 Solvothermal hot-injection (HI) process

OLA (15 mL) was added into a 3-necked round bottom flask attached to a water condenser and evacuated and refilled with N_2 repeatedly using a Schlenk line for *ca.* 15 minutes. When the temperature was at 230 °C, 300 mg of **2b** (dissolved in 5 mL OLA, heated for 15 minutes in an oven at *ca.* 80 °C) was injected into the 3-necked round bottom flask. The colour immediately changed from dark brown to black. The solution was heated to 230 °C and held there for 1 h. The mixture was slowly cooled to room temperature, whereupon MeOH (80 mL) was added with stirring. The mixture was centrifuged, and the solution decanted to give the resultant nanoparticles. This procedure was repeated four times (3 × 80 mL MeOH, 80 mL CH_2Cl_2) and following this the material was air-dried.

4.7 Dry decomposition

Thermolysis was carried out by heating **2b** (placed in a ceramic boat and positioned in the centre of a Carbolite MTF furnace) to 450 °C and kept at this temperature for one hour under argon to produce Cu_xS_y. The final black powders were collected after cooling to room temperature.

Conflicts of interest

There are no conflicts to declare.

Acknowledgements

We thank the Commonwealth Scholarship Commission for a PhD studentship to JCS, King's College London for a PhD studentship to RN and the Chinese Scholarship Council for a PhD studentship to XX. SB thanks the European Commission for the award of a Marie Curie Fellowship (grant no. 893404).

References

1 A. Comin and L. Manna, New Materials for Tunable Plasmonic Colloidal Nanocrystals, *Chem. Soc. Rev.*, 2014, **43**, 3957–3975.
2 C. Coughlan, M. Ibáñez, O. Dobrozhan, A. Singh, A. Cabot and K. M. Ryan, Compound Copper Chalcogenide Nanocrystals, *Chem. Rev.*, 2017, **117**, 5865–6109.
3 L. Chen, H. Hu, Y. Chen, J. Gao and G. Li, Plasmonic $Cu_{2-x}S$ nanoparticles: a brief introduction of optical properties and applications, *Mater. Adv.*, 2021, **2**, 907–926.
4 Y. Liu, M. Ji and P. Wang, Recent Advances in Small Copper Sulfide Nanoparticles for Molecular Imaging and Tumor Therapy, *Mol. Pharmaceutics*, 2019, **16**, 3322–3332.
5 S. Sun, P. Li, S. Liang and Z. Yang, Diversified copper sulfide ($Cu_{2-x}S$) micro-/nanostructures: a comprehensive review on synthesis, modifications and applications, *Nanoscale*, 2017, **9**, 11357–11404.
6 P. Roy and S. K. Srivastava, Nanostructured copper sulfides: synthesis, properties and applications, *CrystEngComm*, 2015, **17**, 7801–7815.
7 A. Agrawal, S. H. Cho, O. Zandi, S. Ghosh, R. W. Johns and D. J. Milliron, Localized Surface Plasmon Resonance in Semiconductor Nanocrystals, *Chem. Rev.*, 2018, **118**, 3121–3207.
8 Y. Liu, M. Liu and M. T. Swihart, Plasmonic Copper Sulfide-Based Materials: A Brief Introduction to Their Synthesis, Doping, Alloying, and Applications, *J. Phys. Chem. C*, 2017, **121**, 13435–13447.
9 A. Shukla, S. Shao, S. Carter-Searjeant, S. Haigh, D. Richards, M. Green and A. V. Zayats, Carrier density tuning in CuS nanoparticles and thin films by Zn doping via ion exchange, *Nanoscale*, 2023, **15**, 3730–3736.
10 J. C. Sarker and G. Hogarth, Dithiocarbamate Complexes as Single Source Precursors to Nanoscale Binary, Ternary and Quaternary Metal Sulfides, *Chem. Rev.*, 2021, **121**, 6057–6123.
11 G. Hogarth, Transition Metal Dithiocarbamates (1978–2003), *Prog. Inorg. Chem.*, 2005, **53**, 71–561.

12 G. Hogarth and D. C. Onwudiwe, Copper dithiocarbamates: coordination chemistry and applications in materials science, biosciences and beyond, *Inorganics*, 2021, **9**, 70.
13 Y. Lou, A. C. S. Samia, J. Cowen, K. Banger, X. Chen, H. Lee and C. Burda, Evaluation of the Photoinduced Electron Relaxation Dynamics of $Cu_{1.8}S$ Quantum Dots, *Phys. Chem. Chem. Phys.*, 2003, **5**, 1091–1095.
14 Y. Wu, C. Wadia, W. Ma, B. Sadtler and A. P. Alivisatos, Synthesis and Photovoltaic Application of Copper(I) Sulfide Nanocrystals, *Nano Lett.*, 2008, **8**, 2551–2555.
15 J. M. Luther, P. K. Jain, T. Ewers and A. P. Alivisatos, Localized Surface Plasmon Resonances Arising from Free Carriers in Doped Quantum Dots, *Nat. Mater.*, 2011, **10**, 361–366.
16 Q. Tian, F. Jiang, R. Zou, Q. Liu, Z. Chen, M. Zhu, S. Yang, J. Wang, J. Wang and J. Hu, Hydrophilic Cu_9S_5 Nanocrystals: A Photothermal Agent with a 25.7% Heat Conversion Efficiency for Photothermal Ablation of Cancer Cells in Vivo, *ACS Nano*, 2011, **5**, 9761–9771.
17 B. Li, Q. Wang, R. Zou, X. Liu, K. Xu, W. Li and J. Hu, $Cu_{7.2}S_4$ Nanocrystals: A Novel Photothermal Agent with a 56.7% Photothermal Conversion Efficiency for Photothermal Therapy of Cancer Cells, *Nanoscale*, 2014, **6**, 3274–3282.
18 J. Cui, S. Xu, C. Guo, R. Jiang, T. D. James and L. Wang, Highly Efficient Photothermal Semiconductor Nanocomposites for Photothermal Imaging of Latent Fingerprints, *Anal. Chem.*, 2015, **87**, 11592–11598.
19 H. Chen, M. Song, J. Tang, G. Hu, S. Xu, Z. Guo, N. Li, J. Cui, X. Zhang, X. Chen and L. Wang, Simultaneous ^{19}F Magnetic Resonance Imaging and Photothermal Therapy, *ACS Nano*, 2016, **10**, 1355–1362.
20 P. B. Mann, I. J. McGregor, S. Bourke, M. Burkitt-Gray, S. Fairclough, M. T. Ma, G. Hogarth, M. Thanou, N. Long and M. Green, An Atom Efficient, Single-Source Precursor Route to Plasmonic CuS Nanocrystals, *Nanoscale Adv.*, 2019, **1**, 522–526.
21 A. R. Hendrickson, R. L. Martin and N. M. Rohde, Dithiocarbamates of Cu(I), Cu(II), and Cu(III). An Electrochemical Study, *Inorg. Chem.*, 1976, **15**, 2115–2119.
22 W. J. Newton and B. J. Tabner, Electron spin resonance study of some copper(II) dithiocarbamates and their mixed ligand complexes, *J. Chem. Soc., Dalton Trans.*, 1981, 466–471.
23 S. C. Ball, I. Cragg-Hine, M. G. Davidson, R. P. Davies, A. J. Edwards, I. Lopez-Solera, P. R. Raithby and R. Snaith, Lithium intermediates during the α-lithiation and subsequent α-substitution of heterocyclic amines in the presence of CO_2, *Angew. Chem., Int. Ed.*, 1995, **34**, 921–923.
24 J. C. Sarker, R. Nash, S. Boonrungsiman, D. Pugh and G. Hogarth, Diaryldithiocarbamates: synthesis, oxidation to thiuram disulfides, Co(III) complexes $[Co(S_2CNAr_2)_3]$ and use as single source precursors to CoS_2, *Dalton Trans.*, 2022, **51**, 13061–13070.
25 H. Michaels, M. J. Golomb, B. J. Kim, T. Edvinsson, F. Cucinotta, P. Waddell, M. R. Probert, S. J. Konezny, G. Boschloo, A. Walsh and M. Freitag, Copper coordination polymers with selective hole conductivity, *J. Mater. Chem. A*, 2022, **10**, 9582–9591.
26 F. W. B. Einstein and J. S. Field, Copper(II) bis(*N*,*N*-dimethyldithiocarbamate), *Acta Crystallogr., Sect. B: Struct. Sci.*, 1974, **B30**, 2928–2930.
27 G. Hogarth, A. Pateman and S. P. Redmond, Crystal structures of copper(III) dithiocarbamate complexes $[Cu(\eta^2\text{-}S_2CNMe_2)_2][ClO_4]$ and $[Cu(\eta^2\text{-}S_2CNEt_2)_2][FeCl_4]$ with and without anion–cation interactions, *Inorg. Chim. Acta*, 2000, **306**, 232–236.
28 G. Hogarth, C.-R. Ebony-Jewel and I. Richards, Functionalised dithiocarbamate complexes: synthesis and molecular structures of bis (2-methoxyethyl) dithiocarbamate complexes $[M\{S_2CN(CH_2CH_2OMe)_2\}_2]$ (M = Ni, Cu, Zn) and $[Cu\{S_2CN(CH_2CH_2OMe)_2\}_2][ClO_4]$, *Inorg. Chim. Acta*, 2009, **362**, 1361–1364.
29 K. Brown, Bis(N-pyrrolidyldithiocarbamato)copper(III)-perchlorate, *Cryst. Struct. Commun.*, 1979, **8**, 157–158.
30 R. Hesse, *Crystal structure of copper(I) diethyldithiocarbamate and its interpretation-an application of chemical topology*. *Ark. Kemi*, 1963, 20, 481.
31 D. Cardell, G. Hogarth and S. A. Faulkner, A dithiocarbamate-stabilized copper(I) cube, *Inorg. Chim. Acta*, 2006, **359**, 1321–1324.
32 A. C. Lane, M. V. Vollmer, C. H. Laber, D. Y. Melgarejo, G. M. Chiarella, J. P. Fackler Jr, X. Yang, G. A. Baker and J. R. Walensky, Multinuclear copper(I) and silver(I) amidinate complexes: Synthesis, luminescence, and CS_2 insertion reactivity, *Inorg. Chem.*, 2014, **53**, 11357–11366.
33 P. V. V. N. Kishorea, D.-R. Shia, J. H. Liao, A. K. Gupta and C. W. Liu, Synthesis and structural characterization of xanthate ligated hydrido Cu(I) clusters and Cu(I) coordination polymer, *Inorg. Chim. Acta*, 2019, **496**, 119068.
34 K. Tang, X. Jin, Y. Long, P. Cui and Y. Tang, Study on the reaction of the anionic copper selenolate complex $[Me_4N]_2[Cu_4(SePh)_6]$ with CS_2 in solvents; the crystal structure of a polymeric complex $[CuS_2COMe]_n$(I), *J. Chem. Res., Synop.*, 2000, 452–453.
35 S. Huang, X. Xu, J. C. Sarker, D. Pugh and G. Hogarth, Primary-amine-derived Cu(I)-dithiocarbamate complexes and their use as low temperature single source precursors to CuS (covellite) nanomaterials. Manuscript in preparation.
36 C. Kowala and J. M. Swan, IB metals. III. Triethyl- and triphenylphosphine complexes of cuprous, argentous, and aurous *NN*-dialkyldithiocarbamates, *Aust. J. Chem.*, 1966, **19**, 555–559Coordination compounds of Group.
37 L. Xu, *N*,*N*-bispropyldithiocarbamato bis(triphenylphosphine) copper(I) dichloromethane solvate: $[\{(n\text{-}Pr)_2dtc(PPh_3)_2\}Cu\cdot CH_2Cl_2]$ (dtc = dithiocarbamate), *Pol. J. Chem.*, 2001, **75**, 755–757.
38 A. N. Gupta, V. Singh, V. Kumar, L. B. Prasad, M. G. B. Drew and N. Singh, Syntheses, crystal structures and optical properties of heteroleptic copper(I) dithio/PPh_3 complexes, *Polyhedron*, 2014, **79**, 324–329.
39 A. Okuniewski, D. Rosiak, K. Chojnacki and B. Becker, Coordination polymers and molecular structures among

complexes of mercury(II) halides with selected 1-benzoylthioureas, *Polyhedron*, 2015, **90**, 47–57.

40 S. Khalid, E. Ahmed, M. Azad Malik, D. J. Lewis, S. Abu Bakar, Y. Khan and P. O'Brien, Synthesis of Pyrite Thin Films and Transition Metal Doped Pyrite Thin Films by Aerosol-Assisted Chemical Vapour Deposition, *New J. Chem.*, 2015, **39**, 1013–1021.

41 N. Hollingsworth, A. Roffey, H. U. Islam, M. Mercy, A. Roldan, W. Bras, M. Wolthers, C. R. A. Catlow, G. Sankar, G. Hogarth and N. H. De, Leeuw, Active Nature of Primary Amines during Thermal Decomposition of Nickel Dithiocarbamates to Nickel Sulfide Nanoparticles, *Chem. Mater.*, 2014, **26**, 6281–6292.

42 A. Roffey, N. Hollingsworth, H. U. Islam, W. Bras, G. Sankar, N. H. De Leeuw and G. Hogarth, Fe(II) and Fe(III) Dithiocarbamate Complexes as Single Source Precursors to Nanoscale Iron Sulfides: A Combined Synthetic and: In Situ XAS Approach, *Nanoscale Adv.*, 2019, **1**, 2965–2978.

43 H. U. Islam, A. Roffey, N. Hollingsworth, W. Bras, G. Sankar, N. H. De Leeuw and G. Hogarth, Understanding the Role of Zinc Dithiocarbamate Complexes as Single Source Precursors to ZnS Nanomaterials, *Nanoscale Adv.*, 2020, **2**, 798–807.

44 S. J. Coles and P. A. Gale, Changing and challenging times for service crystallography, *Chem. Sci.*, 2012, **3**, 683–689.

45 *CrysAlisPRO*, Oxford Diffraction, Agilent Technologies UK Ltd, Yarnton, England.

46 O. V. Dolomanov, L. J. Bourhis, R. J. Gildea, J. A. K. Howard and H. Puschmann, OLEX2: a complete structure solution, refinement and analysis program, *J. Appl. Crystallogr.*, 2009, **42**, 339–341.

47 L. J. Bourhis, R. J. Gildea, J. A. K. Howard and H. Puschmann, The anatomy of a comprehensive constrained, restrained refinement program for the modern computing environment – Olex2 dissected, *Acta Crystallogr., Sect. A: Found. Crystallogr.*, 2015, **71**, 59–75.

48 G. M. Sheldrick, Crystal structure refinement with SHELXL, *Acta Crystallogr., Sect. C: Cryst. Struct. Commun.*, 2015, **71**, 3–8.